JOURNAL OF CATALYSIS **164,** 16–27 (1996)
ARTICLE NO. 0358

Catalysis by 12-Molybdophosphates

1. Catalytic Reactivity of 12-Molybdophosphoric Acid Related to Its Thermal Behavior Investigated through IR, Raman, Polarographic, and X-ray Diffraction Studies: A Comparison with 12-Molybdosilicic Acid

Claude Rocchiccioli-Deltcheff,* Ahmed Aouissi,* Mohamed M. Bettahar,† Suzanne Launay,‡ and Michel Fournier*[,1]

**Laboratoire de Chimie des Métaux de Transition (URA CNRS 419), Université Pierre et Marie Curie, 4 place Jussieu, 75252 Paris Cedex 05, France;* †*Laboratoire de Chimie du Gaz Naturel, Institut de Chimie, UST H. Boumedienne, Algiers, Algeria; and* ‡*Laboratoire de Cristallochimie du Solide (URA 1388), Université Pierre et Marie Curie, 4 place Jussieu, 75252 Paris Cedex 05, France*

Received June 19, 1995; revised May 20, 1996; accepted May 28, 1996

The thermal behavior of 12-molybdophosphoric acid ($PMo_{12}H$) was investigated using coupled techniques (IR and Raman spectroscopies, polarography, X-ray diffraction, and catalytic reactivity in methanol oxidation) and compared with results obtained with 12-molybdosilicic acid. The decomposition of $PMo_{12}H$ occurs in a wide temperature range, leading to mixtures of β- and α-MoO_3. A great analogy between the P and Si compounds is evidenced outside the decomposition range. The differences inside this range (wide for P, narrow for Si compound) are discussed in terms of kinetics of decomposition, textural evolution, and capability to rebuild the Keggin unit. © 1996 Academic Press, Inc.

INTRODUCTION

From some decades the acidic and oxidizing properties of[1] 12-molybdophosphoric acid ($H_3PMo_{12}O_{40}$) have been used in the field of catalysis, in fundamental and applied research (1). Many catalytic reactions are performed at relatively high temperatures (often >350°C), and it is necessary to use a catalyst that is stable under these thermal conditions. However, if this is not the case, the compound can act as a precursor of an active species. Anyway, the knowledge of the thermal behavior of the starting material is of importance. The study of the thermal stability of the title compound has been reported for a long time by many teams using several techniques (in the early phases, essentially thermogravimetry (TG) and differential thermal analysis (DTA)). It is not our purpose to recall all the papers about this now well-known problem: a classical scheme of the thermal evolution under dynamic heating is now generally accepted. The stability range of the anhydrous acid does not depend on the number of molecules of crystallization water (29–30 or 13–14) in the starting compound. Under dynamic heating (thermogravimetric analysis with gas flowing) the anhydrous acid is observed between 140 and 270°C. At higher temperatures, protons come off with oxygen atoms from the polyanion (1.5 H_2O, usually called "constitution water"). Above 450°C, the Keggin structure is completely destroyed, as evidenced by X-ray diffraction (XRD) and IR characterizations (molybdenum trioxide formation). Another method of study is performed by submitting the 12-molybdophosphoric acid to thermal treatments at different temperatures with different durations: this is particularly important for catalytic applications. The nature of the products formed during this thermal evolution has been tentatively elucidated by using different physicochemical techniques such as XRD, ^{31}P-NMR, IR, and Raman (2 and references cited in all the papers). The existence of an anhydride, also called anhydrous KU (Keggin unit), or KU with oxygen vacancies, which could be responsible for the catalytic activity in a narrow range of temperature has been postulated by different authors (2d, 3a–3d). However, this anhydride phase, which is expected to be very unstable, has not really been evidenced: it seems probable that some XRD results (2d) could be interpretated rather as a molybdenum oxide phase (see Section 2.1.3), which is consistent with already proposed assumptions (the formation of oxide clusters as decomposition products has been proposed by several authors: see for instance (3e)). It could be of great interest to elucidate the true nature of the products formed during the thermal treatments in order to explain some differences between phosphorus and silicon compounds.

Moreover, catalytic reactivity studies of methanol conversion in the presence of oxygen (test reaction), coupled with IR spectrometry measurements, were proved to be very sensitive means of probing the changes induced by

[1] Present address: Laboratoire de Catalyse hétérogène et homogène oât C3, USTL, 59655 Villeneuve d'Aso, France.

0021-9517/96 $18.00

thermal treatments in the cases of unsupported and silica-supported 12-molybdosilicic acid (4). Particularly in the case of unsupported samples, a good correlation between the thermogravimetric analysis and the reactivity was evidenced. The reaction changes from acidic to oxidizing in character when the heteropolyacid (HPA) is transformed into molybdenum trioxide. Many works claim that the thermal stability and the acidic properties increase when Si(IV) is replaced by P(V) in the Keggin cage (1b and references therein). On the other hand, it is well known that $H_3PMo_{12}O_{40}$ has in solution a more positive redox potential than $H_4SiMo_{12}O_{40}$ (5). As a consequence, it could be expected that the use of $H_3PMo_{12}O_{40}$ could provide a more efficient catalyst in the methanol oxidation. However, some previous studies (2c, 6, 7a) seem to prove that $H_3PMo_{12}O_{40}$ is not significantly more stable than $H_4SiMo_{12}O_{40}$. It was thus interesting to reinvestigate the thermal behavior of the title compound using coupled techniques such as vibrational spectrometry (IR and Raman), polarography, X-ray diffraction, and catalytic reactivity in methanol conversion in the presence of oxygen.

1. EXPERIMENTAL

1.1. Preparation

12-Molybdophosphoric acid, $H_3PMo_{12}O_{40} \cdot 13H_2O$ (abbreviated $PMo_{12}H$), was prepared according to a method previously described (7a). Purity was checked by thermogravimetry, IR, Raman, polarography (7a), and ^{31}P-NMR (7b).

1.2. Thermal Treatments

For infrared, Raman, and X-ray diffraction studies, the samples (about 500 mg) were heated in air at different temperatures between 140 and 500°C and maintained at each temperature for 3 h. After the sample cooled in a dessiccator, the physicochemical characterizations were performed (the samples were handled in air, without special precautions against atmospheric moisture). In some cases, special exposure to saturated water vapor was carried out after the thermal treatments. For reactivity studies, the samples were heated under He/O_2 flow (80/20) at different temperatures between 140 and 500°C for 2 h before the admission of methanol (see below).

1.3. Physicochemical Techniques

1.3.1. Infrared spectrometry. Infrared spectra were recorded on an IFS66V Bruker FTIR interferometer (4000–220 cm^{-1}, resolution 4 cm^{-1}) as KBr pellets.

1.3.2. Raman spectrometry. Raman spectra were run on a U 1000 Jobin et Yvon spectrometer equipped with a Coherent Innova 70 argon laser (514.5 nm, 100 mW). Rotating-sample techniques were used to prevent decomposition and/or reduction by the laser beam. Powdered samples were pressed in a matrix and rotated at about 1000 rpm.

1.3.3. X-ray diffraction. The XRD powder patterns were recorded on a Philips diffractometer using Cu $K\alpha$ radiation.

1.3.4. Surface area measurements. Nitrogen/helium (molar ratio 0.3) adsorption–desorption isotherms were measured using a Quantasorb Jr. apparatus. All the treated samples (about 300 mg) were in addition pretreated at 150°C at atmospheric pressure prior to the measurements by the BET method (adsorption at 77 K).

1.3.5. Polarographic measurements. The samples were characterized on a Tacussel PRG3 three-electrode apparatus using a rotating glassy carbon electrode (carbon Tokaï) as the working electrode and a saturated calomel electrode (SCE) as the reference electrode. Measurements were performed after each thermal treatment, both before and after the catalytic test. Each treated sample was dissolved in aqueous 1 *M* HCl/dioxan mixture (50/50 v/v) (30 mg of sample into 50 ml solution, i.e., a concentration of around $2\text{–}3 \times 10^{-4}$ *M*). Under these conditions the $PMo_{12}O_{40}^{3-}$ anion exhibits three reversible bielectronic waves in the +0.8- to −0.1-V range [$E_{1/2}$: +0.31 V (2F), +0.18 V (2F), −0.05 V (2F)].

1.3.6. Catalytic measurements. Conversion of methanol in the presence of oxygen was used as a test reaction. Catalytic activities and selectivities were measured with a continuous-flow fixed bed reactor under atmospheric pressure. The catalyst (100 mg), packed in a glass reactor, was preconditioned under He/O_2 flow (mixture 80/20, rate 74 ml/mn) for 2 h at different temperatures. After the pretreatment, the reagent mixture He/O_2/MeOH (85.2/10.3/4.5 mol%) was introduced into the reactor (introduction of MeOH was carried out automatically and continuously by microinjection through a syringe). The reaction was conducted at 240°C. Reaction products were analyzed on line by gas-phase chromatography (apparatus Carlo Erba MFC 500), using flame ionization and catharometer detectors (columns filled with Porapak Q and/or molecular sieve). With the exception of the results concerning the influence of time on the conversion and the selectivities, all the data given were obtained after 18 h of reagent mixture flow at the reaction temperature. Selectivities and activities are expressed as already explained (8).

2. RESULTS

A number of physicochemical characterizations are used to follow the evolution of the 12-molybdophosphoric acid as a function of the temperature of the pretreatments before and after the catalytic reaction. Preliminary results have already been reported in a paper devoted to un-

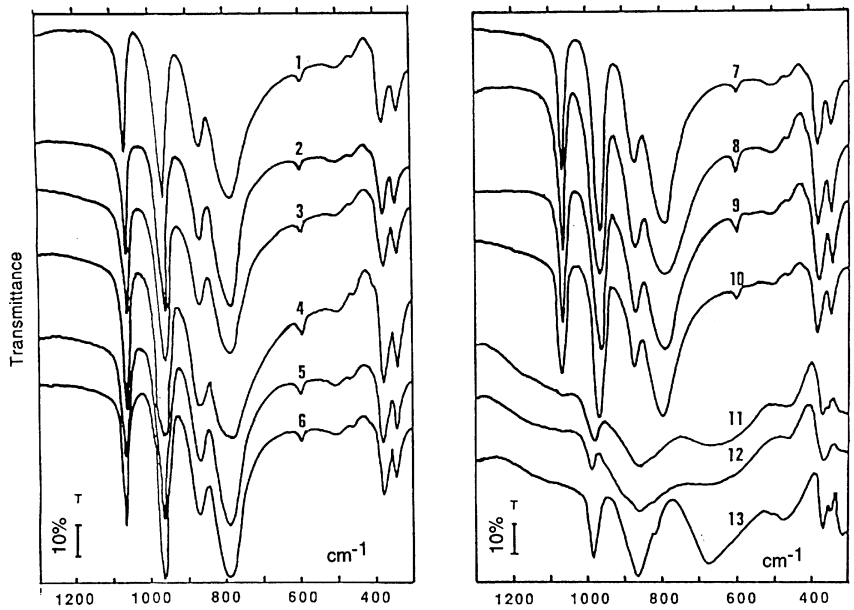

FIG. 1. IR spectra of 12-molybdophosphoric acid. 1, Before any treatment; 2 to 13, after pretreatments at different temperatures (2, 145°C; 3, 200°C; 4, 245°C; 5, 280°C; 6, 300°C; 7, 320°C; 8, 340°C; 9, 360°C; 10, 380°C; 11, 400°C; 12, 440°C; 13, 500°C).

supported and supported 12-molybdophosphoric acid catalysts (9).

2.1. Characterizations before the Catalytic Reaction

2.1.1. Infrared characterizations. IR spectra of the samples before the catalytic reaction are shown in Fig. 1. The spectrum of the untreated $PMo_{12}H$ (Fig. 1, line 1) is consistent with the previously published results (6, 7a). The main characteristic features of the Keggin structure are observed at 1064 cm^{-1} (ν_{as} P–O_a), at 962 cm^{-1} (ν_{as} Mo–O_d), at 869 cm^{-1} (ν_{as} Mo–O_b–Mo), at 787 cm^{-1} (ν_{as} Mo–O_c–Mo), and at 378 and 341 cm^{-1} (bending vibrations) (O_a, oxygen atom bound to 3 Mo atoms and the central P atom; O_b and O_c, bridging oxygen atoms; O_d, terminal oxygen atoms). As seen in Fig. 1, the thermal treatments up to 380°C do not induce significant modifications: the typical features of the Keggin structure are always observed, with only small shifts of the frequencies and general broadening of the bands. A deep modification is evidenced from 400°C, leading progressively to Mo-oxo species closely resembling the orthorhombic molybdenum trioxide, referred to as α-MoO_3 (see Fig. 1, line 13).

2.1.2. Raman characterizations. The Raman spectra of the samples before catalytic reaction are shown in Fig. 2. The spectrum of the untreated $PMo_{12}H$ (Fig. 2, line 1) is consistent with the previously published results (7a). The main characteristic features of the Keggin structure are observed at 998 cm^{-1} (ν_s Mo–O_d), 975 cm^{-1} (ν_{as} Mo–O_d), 909–876 cm^{-1} (ν_{as} Mo–O_b–Mo), 603 cm^{-1} (ν_s Mo–O_c–Mo), and 251 cm^{-1} ("ν_s Mo–O_a," with an important bridge stretching character). After thermal treatments up to 380°C (Fig. 2, lines 2–4), the Raman spectra of $PMo_{12}H$ are always observed, with only small modifications, especially in the spectral region around 900 cm^{-1}. This region is usually related to stretching vibrations of the bridges between two trimolybdic groups of the Keggin structure (ν_{as} Mo–O_b–Mo): these vibrations are sensitive to the dehydration process induced by the thermal treatments (6 and references therein). After the treatment at 380°C, two additional weak bands appear at 775 cm^{-1}, which could be assigned to a monoclinic molybdenum oxide referred to as β-MoO_3, first described by McCarron by means of XRD and Raman spectroscopy as an analogue of WO_3 (10a). From 400°C, the $PMo_{12}H$ pattern completely disappears (Fig. 2, lines 5–7). The spectra displayed in Fig. 2, (lines 5 and 6) are consistent with a mixture of the two oxides α-MoO_3 and β-MoO_3. This interpretation will be explained in more detail below. After treatment at 500°C, only the orthorhombic form of the molybdenum trioxide β-MoO_3 is evidenced (Fig. 2, line 7). In addition, to check the role of water in the composition of the samples after thermal treatment, $PMo_{12}H$ treated at 400°C was exposed to saturated water vapor for several days: the spectrum shown in (Fig. 2, line 8) is consistent with a mixture of α-MoO_3 and $PMo_{12}H$ (β-MoO_3 completely disappears).

2.1.3. X-ray diffraction. The starting material presents the XRD powder diagram of the triclinic 13–14 hydrate of $PMo_{12}H$ (2c, 11). The diagrams of the samples treated at different temperatures are poorly defined: as a consequence only a few interplanar spacings can be measured with a relatively low precision. The sample treated at 380°C exhibits

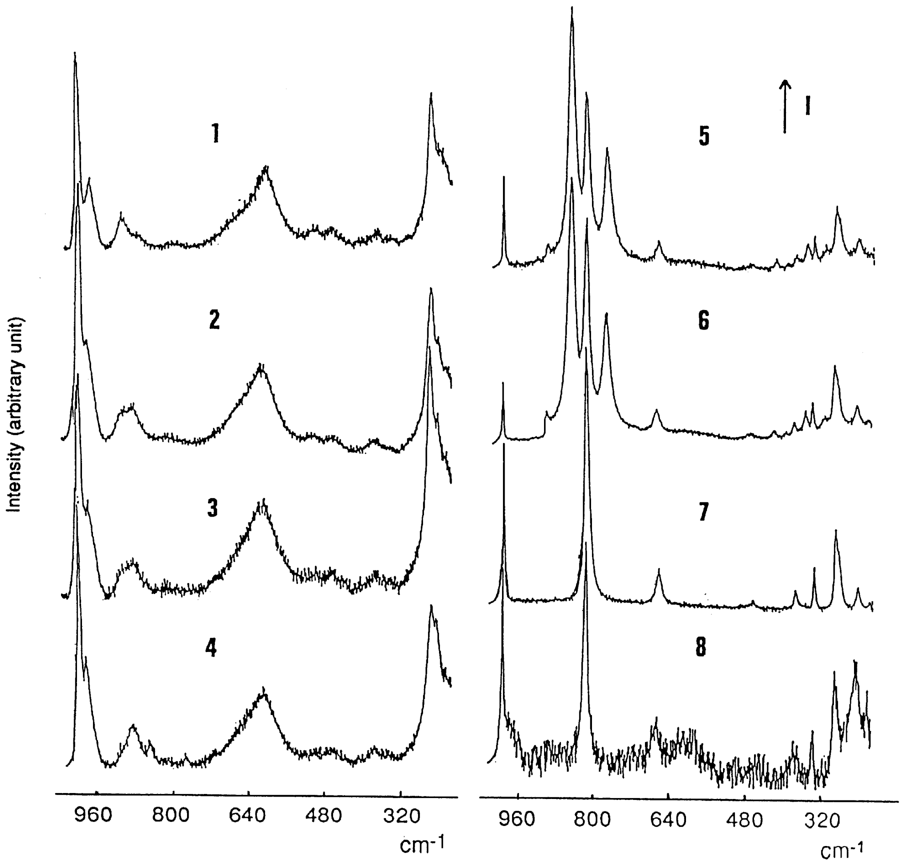

FIG. 2. Raman spectra of 12-molybdophosphoric acid. 1, Before any treatment; 2 to 7, after pretreatments at different temperatures (2, 300°C; 3, 360°C; 4, 380°C; 5, 400°C; 6, 440°C; 7, 500°C); 8, sample treated at 400°C and then exposed to water vapor.

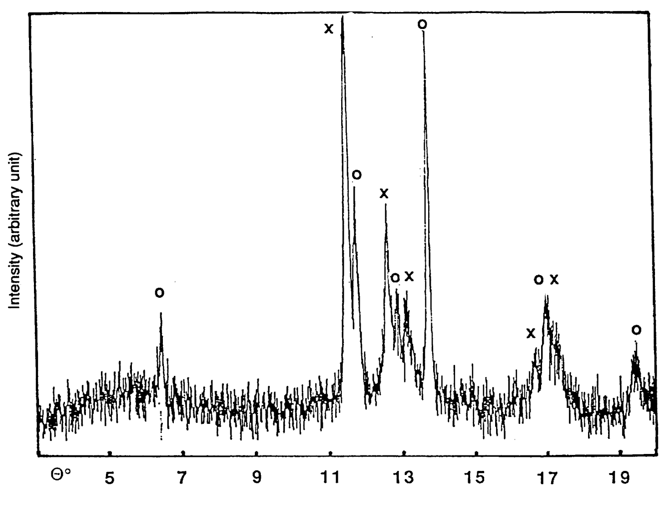

FIG. 3. XRD diagram of 12-molybdophosphoric acid treated at 400°C (similar diagram for the sample treated at 440°C). ○, Lines of α-MoO_3; ×, lines of β-MoO_3.

a pattern which can be related to the tetragonal form of the anhydrous acid (2c), without any line of molybdenum trioxide. For the samples treated at 400 and 440°C (Fig. 3), the features can be related to the most intense lines of the two oxides mentioned above: orthorhombic α-MoO_3 (12) and monoclinic β-MoO_3 (10). The monoclinic form has been reported by several authors, sometimes mixed with other oxides as Mo_4O_{11} and/or α-MoO_3 (10a, b, c, d). Our results compared with the already published data on α-MoO_3 and β-MoO_3 are listed in Table 1. Observation of both Raman and XRD features of β-MoO_3 is consistent with the presence of this species in our samples. After treatment at 500°C, only lines characteristic of α-MoO_3 are observed in the XRD diagram. In a paper devoted to the phase composition of products of thermal decomposition of 12-molybdophosphoric acid, Bondareva *et al.* (2d) give X-ray diffraction data consisting of a list of interplanar spacings, without any correlation with the d_{hkl} of known and/or new phases (lack of crystalline data and cell dimensions): some of these spacings are assigned to the anhydride phase $PMo_{12}O_{38.5}$. However, this is a misinterpretation, because these values closely resemble those of the monoclinic β-MoO_3 oxide.

TABLE 1

Interplanar Spacings d_{hkl} (Å) and Relative Intensities of Orthorhombic α-MoO_3 (Ref. 12) and Monoclinic β-MoO_3 (Refs. 10a, 10b, 10c): Comparison with the XRD Patterns of $PMo_{12}H$ Treated at 400 and 440°C and Proposed Assignments

hkl (Å)	α-MoO_3 Calc.	α-MoO_3 Obs.	*I*%	
200	6.927	6.942	48	
101	3.810	3.808	48	
400	3.464	3.462	60	
210	3.261	3.260	100	
111	2.653	2.653	21	
600	2.308	2.308	33	
	β-MoO_3			
	Ref. 10a	Ref. 10b	Ref. 10c	*I*%
011	3.864	3.860	3.864	100
200	3.559	3.559	3.559	89
−111	3.427	3.428	3.431	27
111	3.364	3.359	3.362	23
020	2.687	2.683	2.683	19
−102	2.619	2.619	2.624	25
211	2.588	2.601	2.586	20
102	2.562	2.572	2.562	16
	$PMo_{12}H$ treated at 400 and 440°C	*I*%	Proposed assignments	
200	6.85	25	α-MoO_3	
011	3.86	100	β-MoO_3	
101	3.76	58	α-MoO_3	
200	3.53	52	β-MoO_3	
400 (α); −111(β)	3.45	32	$\alpha+\beta$-MoO_3	
111	3.37	30	β-MoO_3	
210	3.24	98	α-MoO_3	
020	2.68	19	β-MoO_3	
111(α); −102(β)	2.63	32	$\alpha+\beta$-MoO_3	
211	2.59	25	β-MoO_3	
600	2.31	22	α-MoO_3	

2.1.4. Surface area measurements. Only small changes of the surface areas are observed when the samples are treated in air at different temperatures up to 400°C (for each temperature, the measure cell is filled by the air-treated 12-molybdophosphoric acid). When the heteropolyacid (HPA) decomposes into molybdenum trioxide, the surface area decreases (Fig. 4). A similar (but more pronounced) evolution occurs when the measurements are performed on the same sample kept in the cell and progressively submitted to the different thermal treatments by increasing the temperature up to 320°C, with a BET measurement between two treatments. In this case the thermal history of the sample is completely different. The tendency of increase of the surface area under thermal treatment before the decomposition could be consistent with an evolution of the texture of the HPA from the well crystallized $13H_2O$ hydrate to a poorly crystallized anhydrous acid. As this behavior is much more marked in the case of the 12-molybdosilicic acid, some differences are expected between the two HPAs in the temperature range of the dynamic equilibria between hydrated and anhydrous compound. Moreover, we can consider that the presence of β-MoO_3 of low surface area ($2.6\ m^2\ g^{-1}$, according to Machiels *et al.* (13)) during the thermal treatment of $PMo_{12}H$ can hinder the increasing evolution of the surface area, explaining the difference between the P and Si compounds in the domain of existence of this oxide.

2.1.5. Polarographic measurements. The samples (about 30 mg) dissolved in 50 ml of the aqueous 1 *M* HCl/dioxan mixture (50/50, v/v) show the typical pattern of the Keggin $PMo_{12}O_{40}^{3-}$ anion when treated up to 380°C (Fig. 5). The wave heights vary as follows: up to 240°C they increase due to the water loss (~10% in weight), in the range 240–280°C they remain constant (measures made after treatments at 240, 260, and 280°C), and then they slowly decrease continuously up to 380°C (~10%) and abruptly collapse at 400°C, proving the complete destruction of the Keggin anion. So the $PMo_{12}O_{40}^{3-}$ anion begins to decompose from 280°C: at this temperature and up to 380°C, the extent of decomposition remains weak and cannot be detected by IR: only small shifts and broadening of the bands are observed, as mentioned above, and the characteristic bands of the products of decomposition are masked by those of the main component.

2.2. Characterizations after the Catalytic Reaction

The above characterizations have allowed us to follow the evolution of $PMo_{12}H$ as a function of the temperature of the thermal pretreatments. It is now important to undertake the same kind of characterizations on the samples used, in addition, to catalyze the methanol conversion in presence of oxygen. This can make it possible to know if the samples

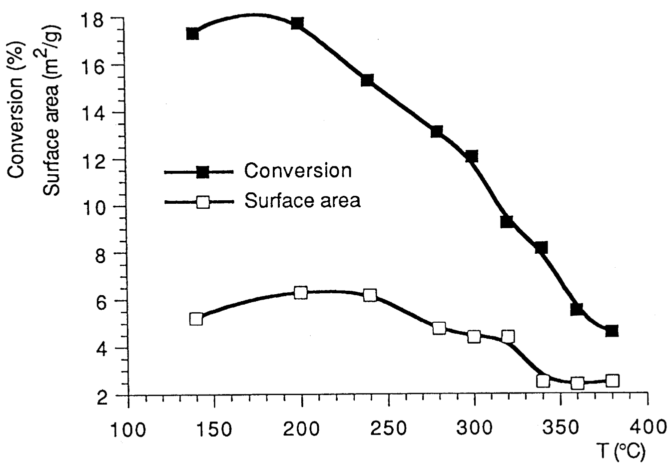

FIG. 4. Variations of surface areas and methanol conversion versus pretreatment temperatures.

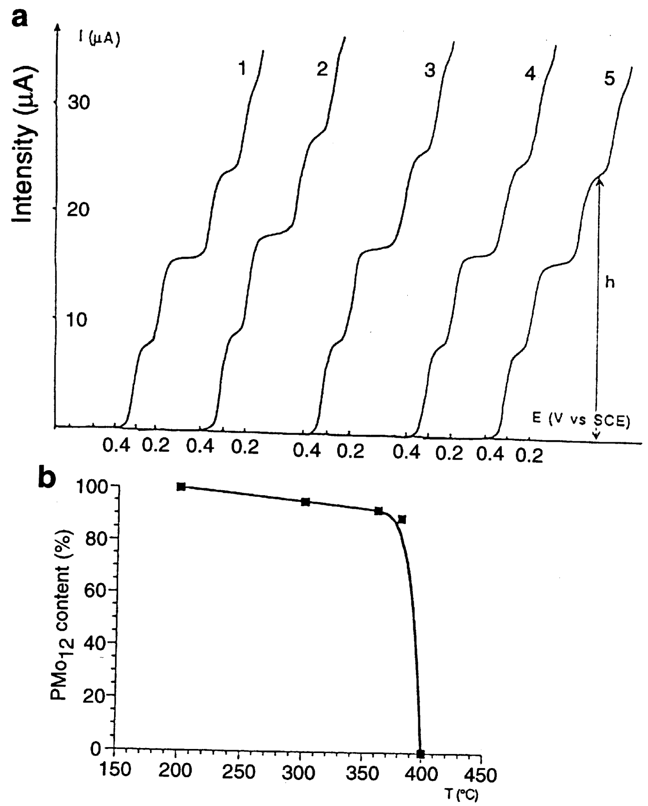

FIG. 5. Polarographic measurements before the catalytic reaction. (a) Polarograms (same sample weight; the heights *h* give a measure of the PMo_{12} content). 1, Before any treatment; 2 to 5, after pretreatments at 200, 300, 360, and 380°C, respectively. (b) PMo_{12} content (%) versus the treatment temperature.

remain unchanged or not during the catalytic reaction for a given pretreatment temperature.

As explained under Experimental, the samples are pretreated for 2 h at different temperatures under He/O_2 flow and then tested at 240°C. At the end of the catalytic reaction, the reactants (O_2 and MeOH) are switched off simultaneously in order to prevent any further evolution of the catalyst, and the samples are characterized by the different physicochemical techniques as above. All the samples undergo a reduction which is more or less pronounced according to the temperature of the pretreatment (color from green to hell and/or deep blue): for pretreatments at temperatures ≤240°C, the samples are greenish and become more and more deeply blue with increasing temperature.

The catalytic reaction does not induce significant changes in the infrared spectra for treatments up to 380°C: the spectra displayed in Fig. 6 are quite similar to those of Fig. 1, with only a broadening of the bands, which may be due to a loss of crystallinity and/or to a partial reduction (14). After treatment at 400°C, followed by the catalytic reaction at 240°C, the IR spectrum is slightly different from that before the reaction (compare Fig. 1, line 11, and Fig. 6, line 10): this could be due to the fact that the samples are mixtures of oxidized and reduced oxides in different proportions. In the temperature range where the Keggin anion is evidenced (Fig. 6, lines 1–9) the IR pattern is very close to that of the oxidized form ($PMo_{12}O_{40}^{3-}$ anion) (14).

Unfortunately, the color of the samples does not permit any measurement of Raman spectra, since the incident beam is absorbed by the reduced sample, as previously reported (15).

For XRD measurements, there are some minor modifications with respect to the samples characterized before the catalytic reaction. When the HPA is not destroyed, the XRD pattern is that of the triclinic $13H_2O$ hydrate, obviously formed from H_2O produced by the reaction or by

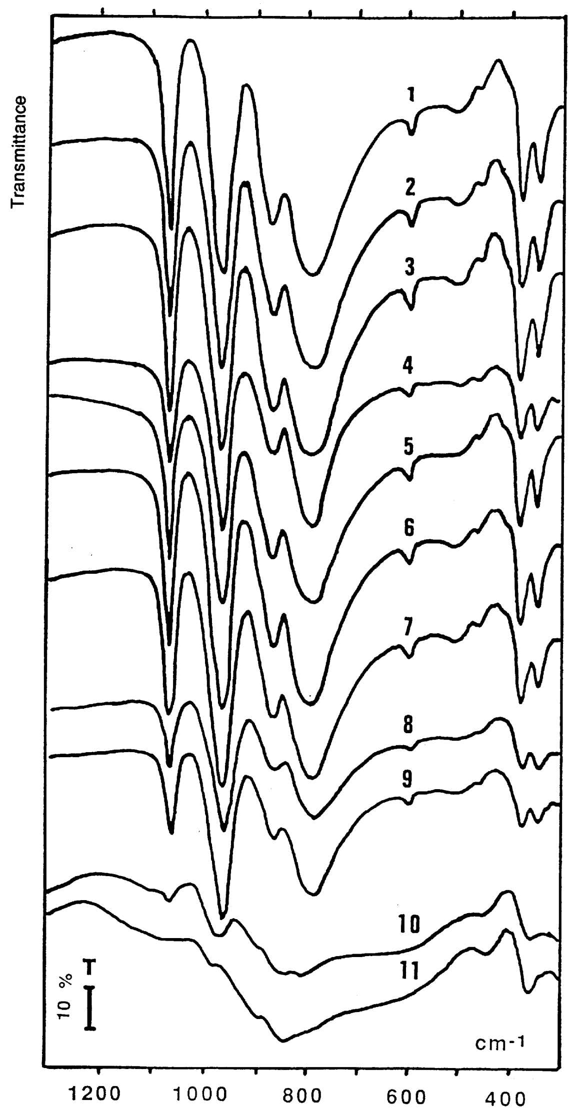

FIG. 6. IR spectra of 12-molybdophosphoric acid pretreated at different temperatures and then tested at 240°C in the methanol oxidation. Pretreatment temperatures: 1, 145°C; 2, 200°C; 3, 245°C; 4, 280°C; 5, 300°C; 6, 320°C; 7, 340°C; 8, 360°C; 9, 380°C; 10, 400°C; 11, 440°C.

fast rehydration since the samples are handled in air. An important diffusion background is observed, especially for the samples treated at temperatures $\geq$280°C: this could be due to a small amount of reduced oxides and/or amorphous phases present in the solid. This is supported by the absence of new lines in the XRD diagram and by the reduction degree from polarographic measurements. Some similar oxides are postulated by Orita *et al.* (16) in order to explain the acetone production in the isopropanol conversion over HPAs.

Only small changes of the surface areas occur, similar to those reported above concerning the measurements before the catalytic reaction, as a function of the pretreatment temperature.

For the polarographic measurements the samples are dissolved in the deaerated aqueous 1 *M* HCl/dioxan mixture as above (no insoluble part for samples treated up to 380°C): the polarograms show the presence of the Keggin $PMo_{12}O_{40}^{3-}$ anion for pretreatment temperatures up to 380°C with quasi constant wave heights (*h* on Fig. 7). A small part of the Keggin anion can be evidenced under a reduced state (about 0.6 e^- for the sample treated at 340°C), which can signify that some part of the sample has been reduced during the reaction. This reduction is clearly shown by the partial translation (h' on Fig. 7) of the first bielectronic waves from the cathodic region toward the anodic one, which is consistent with reversible electrochemical processes (5). Apart this reduction phenomenon, the samples do not present any evolution when submitted to the catalytic reaction up to 380°C, which seems to be in contradiction with the results obtained before the reaction (slow decomposition of the Keggin anion into molybdenum trioxides). This contradiction is apparent only when one considers that the oxide part present in the solid before the reaction could be irreversibly reduced and transformed into reduced HPA by direct synthesis according to the following equation possible in the polarographic cell (aqueous acidic medium) (5):

$$2Mo_4O_{11} + 4MoO_3 + H_3PO_4 + 2H_2O \rightarrow H_7PMo_{12}O_{40}.$$

With this assumption the reduced part evidenced in the polarogram could be a measure of the percentage decomposition of the samples before reaction (i.e., ~10% at 340°C) (the higher the temperature, the higher the amount of the reduced part).

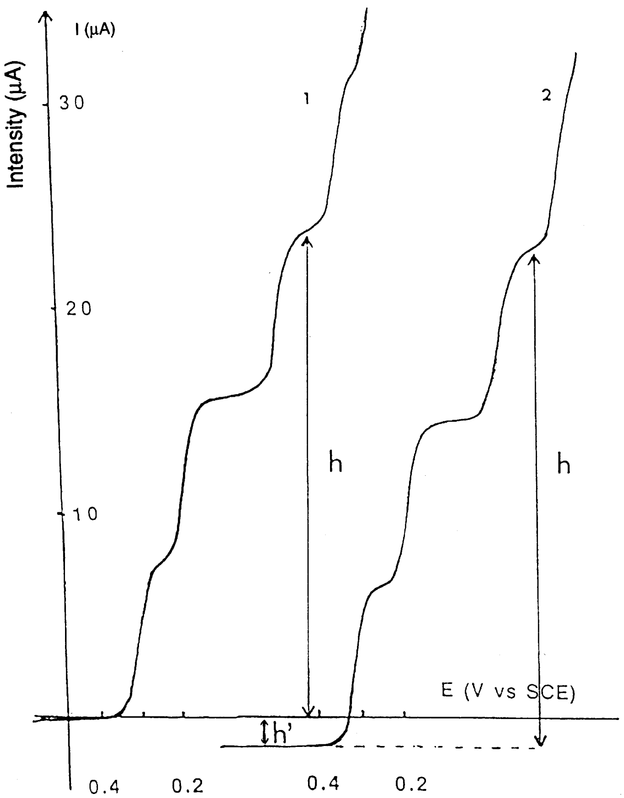

FIG. 7. Polarographic measurements after the catalytic reaction (test conducted at 240°C). Pretreatment temperatures: 1, 200°C; 2, 340°C (*h* corresponds to the PMo_{12} content, h' to the reduced part; see text).

2.3. *Catalytic Reactivity*

The influence of reaction time on the conversion and on the selectivities for the reaction products was checked on samples of $PMo_{12}H$ pretreated at different temperatures for 2 h, the test being conducted at 240°C. The selectivities are rapidly stabilized whatever the pretreatment temperature (see Fig. 8 for three pretreatment temperatures). For pretreatment temperatures less than 280°C, the conversion decreases continuously, showing a tendency to desactivation. For temperatures $\geq$280°C, a steady state is reached after several hours. Similar experiments carried out with the 12-molybdosilicic acid (abbreviated $SiMo_{12}H$) show that the steady state is reached after 8 h of reagent mixture flow, the selectivities for the reaction products being stabilized after ~30 min, as already reported (4). The different behaviors of $PHo_{12}H$ and $SiMo_{12}H$ in terms of conversion as a function of time are illustrated in Fig. 9: it seems that the Si compound evolves more slowly in the time than the P compound. This will be discussed below. The results in the following are given after 18 h of reagent mixture flow.

The variations of the conversion when increasing the pretreatment temperature seem to be correlated with those of the surface area (see Fig. 4), suggesting that the reaction occurs preferentially at the surface.

The results of the catalytic behavior of $PMo_{12}H$ in the methanol oxidation reaction (test conducted at 240°C) after thermal pretreatments at different temperatures are reported in Table 2, Fig. 10 (selectivities) and Figs. 11 and 12 (activities). Three domains of variations of the selectivities as a function of pretreatment temperatures can be evidenced: for temperatures $\leq$240°C, the acidic character

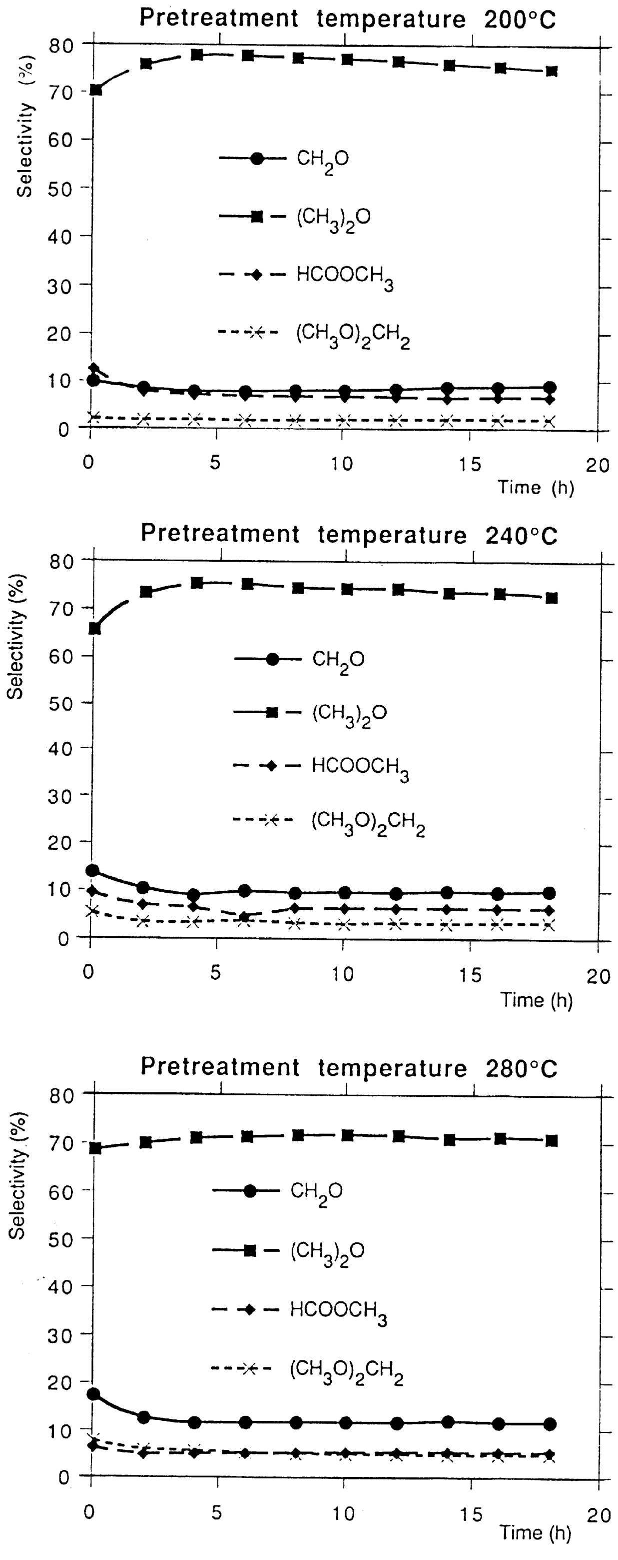

FIG. 8. Catalytic behavior of $PMo_{12}H$ in the methanol oxidation: selectivities as a function of time for three pretreatment temperatures (200, 240 and 280°C).

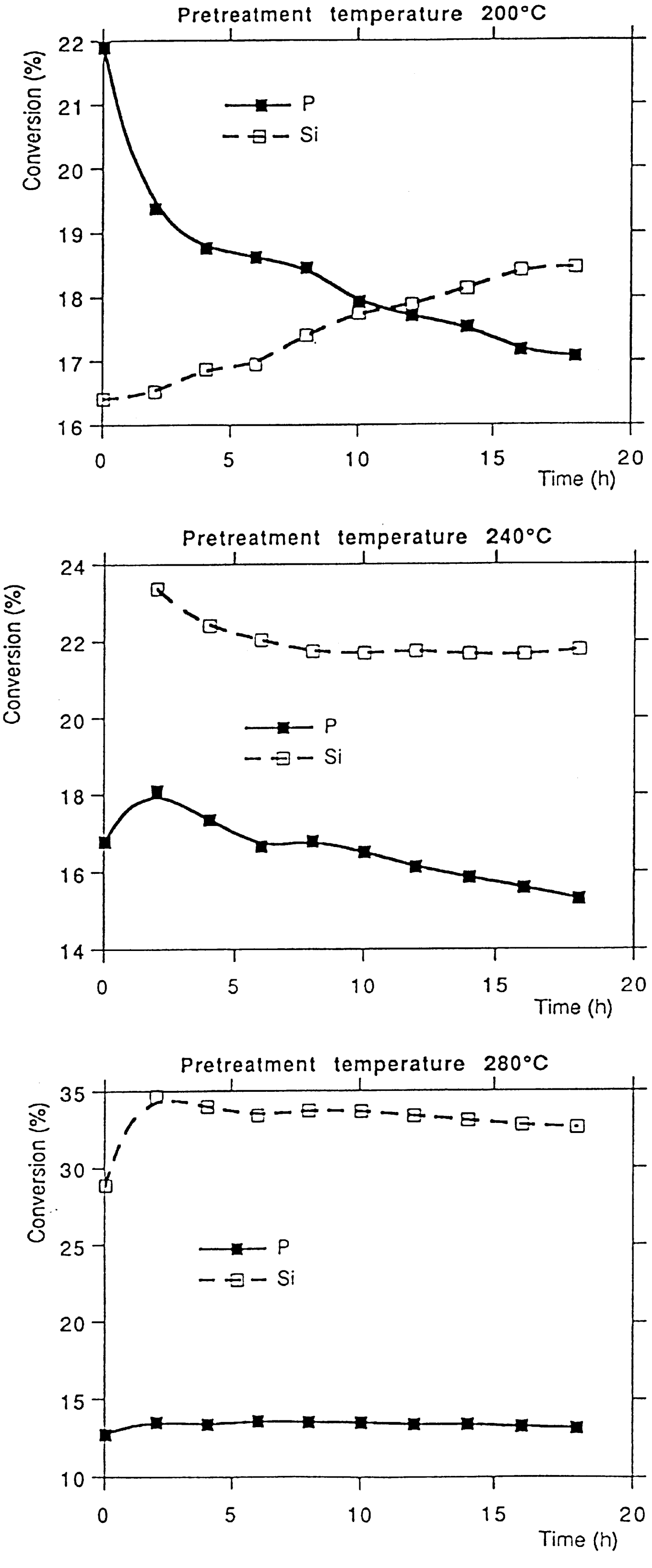

FIG. 9. Comparison of the conversions (%) of $PMo_{12}H$ and $SiMo_{12}H$ as a function of time for three different pretreatment temperatures (200, 240, and 280°C).

TABLE 2

Selectivities and Activities of $PMo_{12}H$ for Methanol Conversion after Thermal Treatments at Different Temperatures (Test Conducted at 240°C)

t (°C)	Conversion (%)	Selectivities[a] (%) 1	2	3	4	5	Total activities (mmol/h/gMo)
140	17	6.9	8.9	75.1	6.7	2.4	39
200	17	8.0	9.0	74.7	6.5	1.8	39
240	15	7.6	10.0	72.8	6.3	3.3	35
280	13	7.7	11.7	70.8	5.2	4.6	30
300	12	8.7	11.4	69.9	5.1	4.9	27
320	9	12.3	12.3	65.5	4.2	5.7	21
340	6	0	17.8	69.6	4.2	8.4	14
360	5	19.3	16.7	53.1	2.7	8.2	12
380	5	24.1	17.3	47.4	2.5	8.7	10
400	7	15.0	53.7	11.8	3.7	15.8	17
440	8	0	77.6	6.1	2.3	14.0	18

[a] 1, CO_2; 2, CH_2O; 3, $(CH_3)_2O$; 4, $HCOOCH_3$; 5, $(CH_3O)_2CH_2$.

remains constant and predominant; for treatments between 260 and 380°C, the selectivity for dimethylether progressively decreases. The reaction remains mainly acidic in character, the redox character being almost constant; for temperatures higher than 400°C, the catalysis character is mainly redox. This behavior is analogous to that of the 12-molybdosilicic acid (4) (Figs. 11 and 12), but the acidic character–redox character transition is performed on a temperature range quite wider (range 280–400°C) than that of $SiMo_{12}H$ (abrupt transition between 300 and 320°C).

3. DISCUSSION

It is now interesting to compare the catalytic behavior of $PMo_{12}H$ and $SiMo_{12}H$. In a previous paper (4), the data collected with $SiMo_{12}H$ were obtained under different conditions related to the different configurations of the reactors

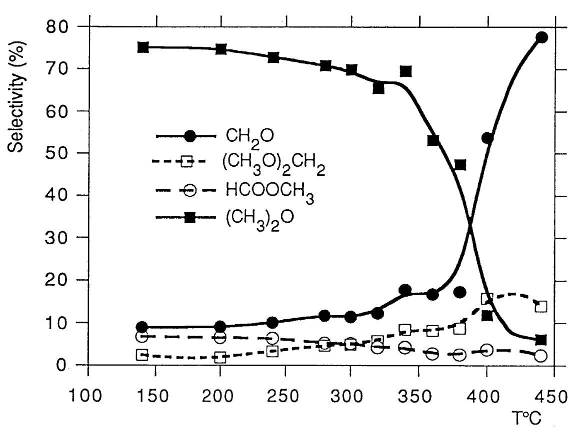

FIG. 10. Catalytic behavior of $PMo_{12}H$ in the methanol oxidation reaction: selectivities as a function of the pretreatment temperatures.

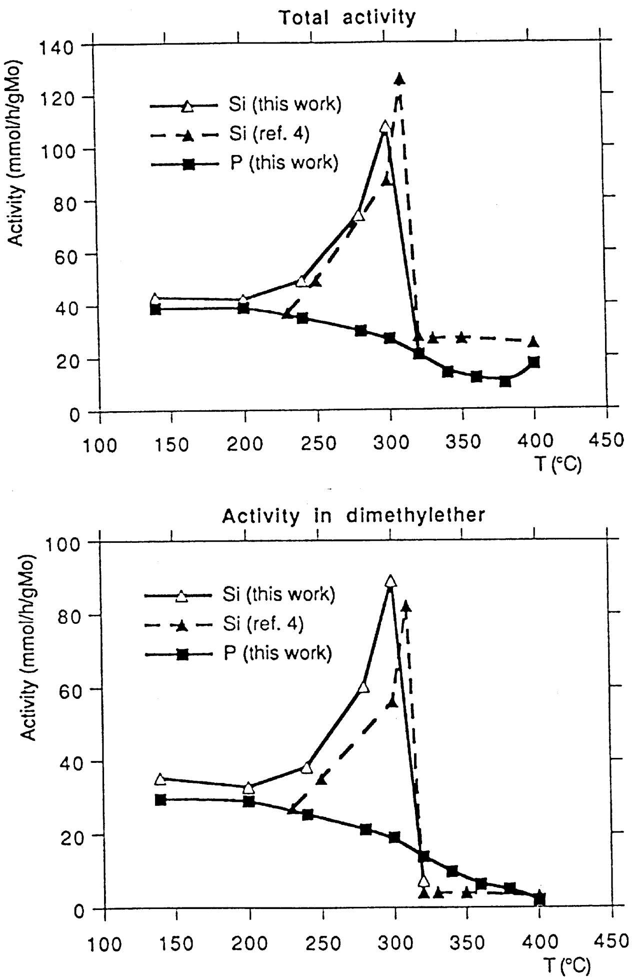

FIG. 11. Comparison of the activities (total activities and activities in dimethylether) in the methanol oxidation reaction as a function of the pretreatment temperatures for $PMo_{12}H$ and $SiMo_{12}H$.

[differences in reaction time (shorter in Ref. 4), amount of catalyst and percentage conversion (lower in Ref.4)]. So we have made again some points for $SiMo_{12}H$ under the same conditions as those used for $PMo_{12}H$. As seen in Fig. 11, the agreement between the data of this work and those of Ref. 4 is reasonable for the total and acidic activities. However, concerning the redox character, expressed as formaldehyde formation, the values from Ref. 4 are higher than those of this work (Fig. 12a). This difference can be understood by taking into account the operating conditions: in this work, the possibility of secondary reactions is greatly favored (longer reaction time, higher amount of catalyst, higher percentage conversion), leading in particular to the transformation of formaldehyde into methyl formate (Fig. 12b). When considering the sum formaldehyde + methyl formate, the agreement is more acceptable (Fig. 12c) and good enough for allowing us to discuss and compare the results and conclusions in all cases.

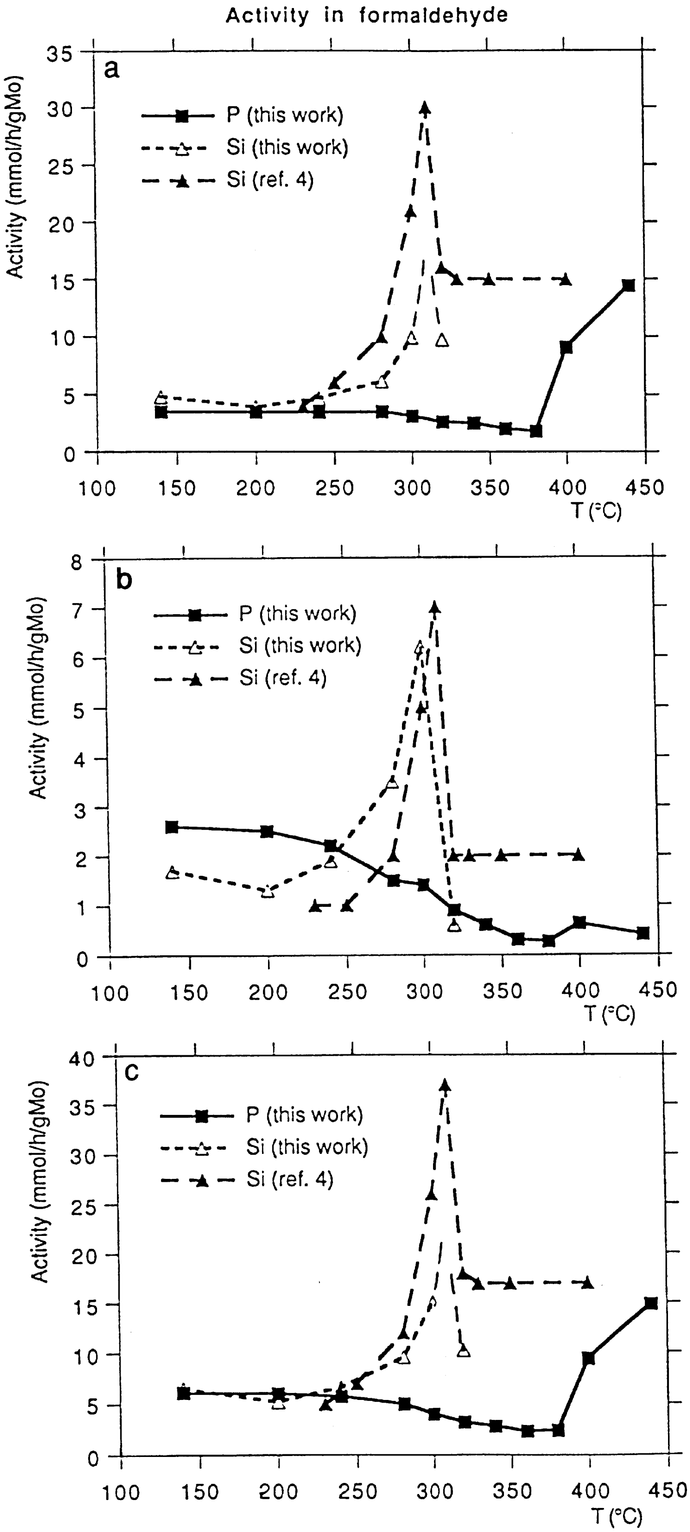

FIG. 12. Comparison of the redox activities in the methanol oxidation reaction as a function of the pretreatment temperatures for $PMo_{12}H$ and $SiMo_{12}H$. (a) Activity in formaldehyde; (b) Activity in methyl formate; (c) Activity in formaldehyde and methyl formate.

It has been generally reported that $PMo_{12}H$ and $SiMo_{12}H$ have rather different behaviors. As seen in Figs. 11 and 12, the results are consistent with this point of view, but only when the 240–320°C temperature range is concerned (in this thermal range, the surface areas of the two compounds are very different). In fact, except for this thermal range, the acidic and redox properties, estimated from dimethylether and formaldehyde production, are rather similar for these two compounds, which have quasi-identical behaviors, in terms of both activity and acidity. This is a very surprising result.

For temperatures ≤240°C, i.e., in a range where the stability of the compounds is clearly evidenced from spectroscopic and electrochemical data, the behaviors are identical and mainly acidic. Above 350°C, $SiMo_{12}H$ is completely transformed into α-Mo_3, and $PMo_{12}H$ is only partially destroyed, with formation of a mixture of α- and β-MoO_3. It seems that β-MoO_3 presents a redox activity lower than that of α-MoO_3. This is consistent with the tendency to increase of the redox character at higher temperatures (≥400°C) in correlation with the progressive transformation of β-MoO_3 into α-MoO_3 (high-temperature phase). When the temperature is high enough to completely transform β-MoO_3 into α-MoO_3, the redox activity is practically the same in both cases (Si or P).

In the 240–320°C temperature range, the great difference between the two compounds is due to the different kinetics of decomposition and to the great influence of the textural evolution on the activity. $SiMo_{12}H$ remains stable up to 300°C (or at least the kinetics of its decomposition is very slow up to 300°C) and then abruptly collapses, giving rise directly to α-Mo_3 at 320°C. Before the decomposition the modification of the texture (increase of surface area) favors the increase of the activity. This evolution is hindered in the case of $PMo_{12}H$, which decomposes progressively in a wide range of temperature (280–350°C). The formation of β-MoO_3, less acidic than $PMo_{12}H$, but presenting similar oxidizing power could explain why the redox character remains almost constant in this range.

The production of water during the reaction can play an essential role on the reactivity. In a temperature range where the thermal pretreatment has affected the heteropolyacid (HPA) only in its hydration state (formation of anhydrous acid), the water produced during the catalytic reaction allows a steady state associating the anhydrous HPA and the 13-hydrate (triclinic phase): this phase is probably responsible for the acidic character through the hydrated protons ($H_5O_2^+$) of the superficial layers of the crystalline lattice. In fact, as shown by Kozhevnikow *et al.* (17), the proton sites in solid HPAs are strongly dependent on the hydration degree: the less hydrated the compounds, the more trapped the protons. Thus this acidic character strongly depends on the surface of the solids: this is understandable if the surface steady state is due to a crystalline microphase of triclinic acid. At higher temperatures, and especially in the decomposition range of the HPA (abrupt for Si and wide for P), the interface composed of HPA not yet decomposed and molybdenum trioxides varies continuously and plays a major role on the reactivity. We have reported above that in the presence of water vapor, $PMo_{12}H$ treated at 400°C (mixture of phosphorus oxide, α-MoO_3, and β-Mo_3) is tranformed into a mixture of $PMo_{12}H$ and α-MoO_3 (Raman spectrum, Fig. 2, line 8): this is possible thanks to the water formed during the catalytic reaction. So the collapse of $PMo_{12}H$ is limited, leading to a quasi-equilibrium,

$$2H_3PMo_{12}O_{40} \Leftrightarrow P_2O_5 + 24\beta\text{-}MoO_3 + 3H_2O,$$

in contrast to the decomposition of $SiMo_{12}H$, which occurs without equilibrium:

$$H_4SiMo_{12}O_{40} \rightarrow SiO_2 + 12\alpha\text{-}MoO_3 + 2H_2O.$$

On the other hand, the correlation between the activity of the products and the surface area does not seem to be consistent with the hypothesis of a pseudo-liquid phase in this particular reaction, as generally admitted (18). However, the meaning of surface in this kind of complicated solid can induce a misunderstanding. It does not seem necessary that alcohol penetrates into the bulk: the polar substrate (water or alcohol) can react with the anhydrous material, resulting in a quasi-homogeneous phase on the surface. Let us remember that surface area evolution occurs in the temperature range of proton elimination. This can imply the modification of the porous system, which can react as a pseudo-liquid phase. Moffat *et al.* (19) have observed that the surface area decreases when the 12-tungstophosphoric acid is submitted to thermal treatments: simultaneously a change in the pore distribution occurs (collapse of the smaller mesopores and increase of the radius of the biggest ones, in the range 70–100 Å). So even if the suface area decreases, the increase of the pore volume could allow better accessibility for the alcohol reagent (the penetration of the reagent into the pore volume could be considered as similar to the penetration into the bulk). From this point of view, this can be considered as a pseudo-liquid phase and the solid-state ^{31}P NMR spectra exhibit very isotropic signals (18). With this assumption, the behaviors of silicon and phosphorus compounds are expected to be very different because there are more available protons in the pseudo-liquid phase for the 12-molybdosilicic acid. However, that is not the observed result, and it seems useful to consider another process. The reaction could be performed at the surface and not in the bulk. This is consistent with results obtained by Mastikhin *et al.* (20) showing the existence of superacid protons in unsupported and silica-supported 12-tungstophosphoric acid. In our case, microdomains of triclinic hydrated phase (with solvated protons) can be formed at the surface of the anhydrous amorphous solid. It seems improbable that the reactant has to migrate into the bulk under these conditions.

The great similarity between these two HPAs shows that the acidic and redox activities are not correlated with the intrinsic behavior of the anions as known from studies in solution. As a matter of fact, the solids do not exhibit any difference, as could be expected from the different numbers of acidic protons and from the different redox potentials. That may be another proof that the reactant MeOH is not present as a liquid phase in the bulk of the material.

4. CONCLUSION

It appears from these results that the conversion of methanol (coupled with physicochemical characterizations) is a useful probe for studying surface phenomena during the thermal decomposition of molybdenum HPAs (12-molybdophosphoric and silicic acids). This study has pointed out the analogies and the differences between these two HPAs and provided evidence of some important effects related to the thermal stability.

If the kinetics of decomposition is slow enough (as in the case of Si), a textural effect is predominant, leading to the increase of the surface area and of the activity with increasing temperature: the decomposition arises quite abruptly in a short range of temperature and leads directly to α-MoO_3.

In the case of the P compound, the kinetics of decomposition is quicker, and this completely modifies the behavior in the wide decomposition range. The tendency to form β-MoO_3 hinders the textural evolution. Moreover, the capability of this oxide to react with the water vapor in the presence of phosphoric oxide to form again the initial HPA plays an essential role.

Outside the decomposition range, a close analogy is evident, between the P and Si compounds: similar acidity and similar redox character. However, the capability of $PMo_{12}H$ to be rebuilt under reaction conditions (from β-MoO_3 in the presence of water vapor produced by the reaction) can explain why the P molybdenum compounds are usually claimed to be more efficient and stable than the Si ones. That may be also the reason for the success of Keggin molybdophosphoric acid derivatives in many reported patents.

ACKNOWLEDGMENTS

The authors thank Professor Michel Che and Dr. Raymonde Franck for providing access to the IFS66V Bruker FTIR spectrometer.

REFERENCES

1. (a) Misono, M., *Catal. Rev. Sci. Eng.* **29**, 269 (1987); *Appl. Catal.* **64**, 1 (1990); (b) Mizuno, M., and Misono, M., *J. Mol. Catal.* **86**, 319 (1994); (c) McMonagle, J. B., and Moffat, J. B., *J. Catal.* **91**, 132 (1985); (c) Kozhevnikov, I. V., *Russ. Chem. Rev.* **56**, 811 (1987); *Catal. Rev. Sci. Eng.* **37**, 311 (1995).

2. (a) Pope, M. T., “Heteropoly and Isopoly Oxometalates.” Springer-Verlag, Berlin, 1983; (b) Tsigdinos, G. A., *Top. Current Chem.* **76**, 1 (1978); (c) Fournier, M., Feumi-Jantou, C., Rabia, C., Hervé, G., and Launay, S., *J. Mater. Chem.* **2**, 971 (1992), (d) Bondareva, V. M., Andrushkevich, T. V., Maksimovskaya, R. I., Plyasova, L. M., Ziborov, A. V., Litvak, G. S., and Detusheva, L. G., *Kinet. Catal.* **35**, 114 (1994).
3. (a) Jerschkewitz, H. G., Alsdorf, E., Fichtner, H., Hanke, W., Jancke, K., and Öhlmann, G., *Z. Anorg. Allg. Chem.* **526**, 73 (1985); (b) Ai, C. D., Reich, P., Schreier, E., Jerschkewitz, H. G., and Öhlmann, G. Z. *Anorg. Allg. Chem.* **526**, 86 (1985); (c) Kasztelan, S., Payen, E., and Moffat, J. B., *J. Catal.*, **125**, 45 (1990) (d) Payen, E., Kasztelan, S., and Moffat, J. B., *J. Chem. Soc. Faraday Trans.* **88**, 2263 (1992); (e) Serwicka, E. M., and Grey, C. P., *Colloids Surf.* **45**, 69 (1990).
4. Rocchiccioli-Deltcheff, C., Amirouche, M., Hervé, G., Fournier, M., Che, M., and Tatibouët, M., *J. Catal.* **126**, 591 (1990).
5. (a) Fournier, M., Thèse de Doctorat ès sciences physiques, University of Paris, 1976; (b) Hervé, G., and Massart, R., *Rev. Chim. Min.* **5**, 501 (1968).
6. Rocchiccioli-Deltcheff, C., and Fournier, M., *J. Chem. Soc. Faraday Trans.* **87**, 3913 (1991).
7. (a) Rocchiccioli-Deltcheff, C., Fournier, M., Franck, R., and Thouvenot, R., *Inorg. Chem.* **22**, 207 (1983); (b) Thouvenot, R., Rocchiccioli-Deltcheff, C., and Fournier, M., *J. Chem. Soc. Chem. Commun.* 1352 (1991).
8. Rocchiccioli-Deltcheff, C., Amirouche, M., Che, M., Tatibouët, M., and Fournier, M., *J. Catal.* **125**, 292 (1990).
9. Fournier, M., Aouissi, A., and Rocchiccioli-Deltcheff, C., *J. Chem. Soc. Chem. Commun.* 307 (1994).
10. (a) McCarron, III, E. M., *J. Chem. Soc. Chem. Commun.* 336 (1986); (b) Harb, F., Gérand, B., Nowogrocki, G., and Figlarz, M., *Compt. Rend. Acad. Sci., Ser. II* **303**, 349 (1986); (c) Svennsson, G., and Kihlborg, L., *React. Solids* **3**, 33 (1987); (d) Parise, J. B., McCarron, III, E. M., Von Dreeler, R., and Goldstone, J. A., *J. Solid State Chem.* **93**, 193 (1991).
11. d’Amour, H., and Allmann, R., *Z. Kristallogr.* **143**, 1 (1976).
12. (a) Andersson, G., and Magnéli, A., *Acta Chem. Scand.* **4**, 793 (1950); (b) Westman, S., and Magnéli, A., *Acta Chem. Scand.* **11**, 1587 (1957); (c) Kihlborg, L., *Ark. Kemi.* **21**, 357 (1963).
13. Machiels, C. J., Cheng, W. H., Chowdhry, U., Farneth, W. E. Hong, F., McCarron, E. M., and Sleight, A. W., *Appl. Catal.* **25**, 249 (1986).
14. Fournier, M., Rocchiccioli-Deltcheff, C., and Kazansky, L. P., *Chem. Phys. Lett.* **223**, 297 (1994).
15. Rocchiccioli-Deltcheff, C., Amirouche, M., and Fournier, M., *J. Catal.* **138**, 445 (1992).
16. Orita, H., Hayakawa, T., Shimizu, M., and Takehira, K., *Appl. Catal.* **77**, 133 (1991).
17. Kozhevnikov, I. V., Sinnema, A., and Van Bekkum, H., *Catal. Lett.* **34**, 213 (1995).
18. Lee, K. Y., Arai, T., Nakata, S-I., Asaoka, S., Okahara, T., and Misono, M., *J. Am. Chem. Soc.* **114**, 2836 (1992).
19. Hayashi, H., and Moffat, J. B., *J. Catal.* **77**, 473 (1982).
20. Mastikhin, V. M., Kulikov, S. M., Nosov, A. V., Kozhevnikov, I. V., Mudrakovsky, I. L., and Timofeeva, M. N. *J. Mol. Catal.* **60**, 65 (1990).